Physica B 520 (2017) 28–36

Contents lists available at ScienceDirect

Physica B

journal homepage: www.elsevier.com/locate/physb

The influences of the properties of impurities and defects on the dark I-V characteristic curve and output parameters of c-Si solar cells

Xiaodong Lu, Yang Song*, Jie Gao, Xinxin Wang, Yufeng Zhang

College of New Energy, Bohai University, Jinzhou 121000, Liaoning, China

ARTICLE INFO

Keywords:
Crystalline silicon cell
Dark I-V characteristic curve
Ideal factor
Impurity
Defect
Output parameter

ABSTRACT

The influences of the coating ratio of electrode, doping concentration of substrate and type of impurities and defects on the dark I-V characteristic curves and output parameters of c-Si solar cells are studied by finite difference method and the dark I-V characteristic curves under different conditions are analyzed by their ideal factors, the results show that: the dark current values under the same bias voltage will increase with the increasing of the coating ratio of electrode or doping concentration of substrate; the influences of donor-like, acceptor-like and recombination-center-like impurities and defects on the dark I-V characteristic curves have threshold effects; the parameters of the impurities and defects smaller than their corresponding threshold will have no obvious influences on dark I-V characteristic curves; the acceptor-like impurities and defects on the surface of c-Si solar cells have no influences on their dark I-V characteristic curve, but the donor-like and recombination-center-like impurities and defects have strong influences on their dark I-V characteristic curve; the variations of the output parameters of c-Si solar cells are analyzed in detail under the different properties of the impurities and defects inside and on the surfaces of c-Si solar cells.

1. Introduction

The dark current-voltage (I-V) characteristic curve of a crystalline silicon solar cell (c-Si SC) is the I-V characteristic curve without illumination. Due to the lack of illumination, the concentration of injected carriers increases with the increasing of forward bias before the pn junction of the c-Si SC conducts, so the injected carrier concentration of the c-Si SC can be effectively controlled by the applied bias voltage [1]. The pn junction properties [2,3], impurity and defect properties [4,5] will produce different responses in the dark I-V characteristic curve with the control of the level of injected carrier by the applied bias voltage, so the dark I-V characteristic curve has been paid more and more attentions by researchers and regarded as a supplementary characterization method in the research of c-Si SCs [6–8].

In the early researches of dark I-V characteristic curves, the main achievement is to correct the diode model errors based on the results obtained by dark I-V characteristic curve, and transform the single diode model into the double diode model [1]. In the double diode model, two equivalent diode models are used to individually connect with the diffusion or generation/ recombination currents inside a c-Si SC, and the influences of the generation and recombination mechanisms of carriers on the dark I-V characteristic curves are analyzed by introducing those corresponding empirical formulas into the double diode model [9,10]. In recent years, the researchers begin to introduce the dark I-V characteristic curve to the detection and analysis of the properties of the impurities and defects inside a c-Si SC because of the increasing requirements of the c-Si SCs with high efficiency in the market and the recognition of the important influences of the properties of the impurities and defects on the cell efficiency. In 2009, O. Breitenstein et al. studied on the influences of surface recombination centers on the dark I-V characteristic curves by adjusting the amount of diamond and changing the damage of silicon wafer surfaces in the slicing process [11]; In 2010, O. Breitenstein et al. further investigated the influence of the mutual coupling between the defects of c-Si SC on the dark I-V characteristic curve by using the double diode model and lock-in thermography (LIT) technique [12]; In 2011, S. Tutashkonko et al. analyzed the electrical properties of electrodes after screen printing Ag and Al electrodes by using the dark I-V characteristic curve [13]. In 2012, L. Derbali et al. investigated the defect state densities in the grain boundaries of a multi-c-Si SC passivated by anti-reflection film by using the dark I-V characteristic curve [14]. In 2014, R.V.K. Chavali et al. studied on the non-ideal dark I-V characteristic curves of a silicon based heterojunction SC in the range of moderate bias of 0.4 V~0.8 V, they pointed out that the defect densities of heterojunction interface is a key factor to induce the non-ideal dark

* Correspondence to: College of New Energy, Bohai University, Jinzhou 121000, Liaoning, China.
E-mail addresses: lxd2211@sina.com (X. Lu), 944560020@qq.com (Y. Song), 876771836@qq.com (J. Gao), 1012421826@qq.com (X. Wang), 459586882@qq.com (Y. Zhang).

http://dx.doi.org/10.1016/j.physb.2017.06.003
Received 27 February 2017; Received in revised form 1 June 2017; Accepted 1 June 2017

I-V characteristic curves [7]. In 2016, P. Somasundaran et al. studied on the influence of shunt resistance on the performance of a industrial c-Si SC by combining the double diode model with lock-in thermography(LIT)technique and pointed out that the efficiency and filling factor of the c-Si SC can be increased by 1–1.5% and 3–4% respectively by reducing the shunt resistance effect of the c-Si SC effectively [8]; In 2016, A.K. Biswas et al. studied on the influence of heavy doping effects on the performance of a c-Si SC by using empirical formulas, and pointed out that the dark current density will increase with the increasing of the doping concentration [15]. In a word, the double diode model is the main tool to study and analyze the dark I-V characteristic curves of c-Si SCs at present, but due to the complex variations of dark I-V characteristic curves, the fundamental laws of the variations of the dark I-V characteristic curves with the properties of the impurities and defection both inside c-Si material and on the surface of c-Si material are still unclear.

Due to assuming uniform distributions of parameters in a cell structure and the simulation results varying obviously with those empirical formula selected, the simulation results of the dark I-V characteristic curves obtained by the double diode model will lead to lager errors sometimes. In the simulation process of semiconductor device characteristic curve, the results of the dark I-V characteristic curve obtained by solving the basic semiconductor device equations by numerical computation method are more accurate than those obtained by the diode model for the reasons that the former only quotes the basic material parameters and few empirical formulas. In addition, the problem of the spatial distributions of the structural parameters can be fully considered in solving the basic semiconductor device equations by numerical computation method [16,17]. This paper will discuss the influence of the electrode form, doping concentration of substrate and properties of impurities and defects on the dark I-V characteristic curve of a c-Si SC by using numerical computation method, and analyze the basic rules of the influence of these factors on the dark I-V characteristic curve.

2. Cell parameter, calculation model and simulation method

2.1. Cell parameter

A typical structure of a c-Si SC is shown in Fig. 1(a) and its main structural units include : active layer (c-Si), double-sided pyramid texture structure, anti-reflection coating (ARC , single layer SiN_x), passivation layer(PL), cathode(Ag cathode) and anode(Al anode). In Fig. 1, H、H_1、H_2 and H_3 represent the height of the texture structure and the thicknesses of the PL layer, Al electrode and ARC, respectively; L, L_0 and L_1 represent the length of the period, Al electrode contact hole and Ag grid electrode, respectively; T+2 H represents the thickness of active layer. In our simulation, the commonly used structure parameters of c-Si SCs are selected [18,19], i.e. H = 7 μm , H_1 = 100 nm , H_2 = 200 nm , H_3 = 70 nm , T = 200 μm , L_0 = 1 μm, respectively. Considering the actual width of the fine grid area of a c-Si SC is about 75 μm and the bottom width of a pyramid L is about 10 μm, so here we denote the period number of pyramid and the number of pyramid covered by electrode by M and N, respectively. For a specific M value , the coverage ratio between the gate electrode and the pyramid structure is represented by the value of S (S = N/M).

In the process of manufacturing a c-Si SC, phosphorus and boron diffusions are often used to create pn junction in the front surface and back field in the back surface, respectively. The conditions for two kinds of diffusion are chosen as [20–22]: for a p type silicon wafer, the phosphorus-diffusion temperature and time are 900 ℃ and 20 min, respectively; the boron-diffusion temperature and time are 900 ℃ and 5 min, respectively. The p type silicon wafer with its substrate concentration of $5\times10^{16}/cm^3$($\rho\approx0.35$ Ω cm) is selected in our simulation. In Fig. 1(b), the Athena module of Silvaco software is used to simulate the distribution of net impurity concentration under the above diffusion conditions. Considering that every pyramid will have a same diffusion impurity distribution under the same diffusion condition, here we selected M=1. In our calculation, uniform grids are adopted and the initial mesh numbers are set to 100 and 800 in the X and Y directions, respectively; The entire grid structure is finally optimized by the Devedit module of Silvaco software (the lengths of initial basic grid in the X and Y directions are all set to 1 μm); The total grid number and triangle-grid number are 9232 and 17447, respectively. As shown by Fig. 1(b), the surface concentration of phosphorus, the junction depth and the square resistance are about $2.97\times10^{20}/cm^3$, 0.59 μm and 38.26 Ω/□, respectively. Fig. 1(b) shows that the net concentration distribution and the junction depth are all not uniform along the X direction under the same diffusion condition; The closer the position the top of the “Pyramid spire”, the greater the concentration and the junction depth.

2.2. Computational model

In the absence of light, the carriers injected by the electrodes and thermally excited are the main source of dark current. Once carriers (electrons and holes) appear, their movement processes in a c-Si material can be divided into two categories, i.e. diffusion and drift movement. Many factors can influence the movement processes of carriers, which can be explained by a simplified energy band diagram of pn junction. Fig. 2 shows the changes of the band structure diagram with different bias voltage, where E_C and E_V represent the energy level at the bottom of the conduction band and on the top of the valence band, respectively; E_F represents the Fermi level. Considering the injection, excitation and recombination processes of electron and hole have a similar mechanism (the direction of increased energy for holes is opposite to that for electrons), Fig. 2 only offer the transport processes related to electron. In order to simplify our discussion, we only take the transport process of electrons as an example to investigate the transport processes of electron and hole. Under a certain temperature,

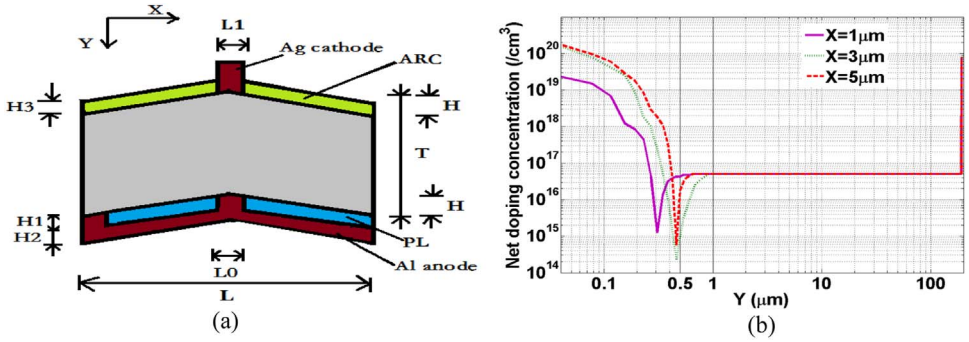

Fig. 1. (a) A typical structure of a c-Si SC and (b) net doping concentration distribution , where X denote the line passing through point (X,Y=0) and parallel with Y axis give by Fig. 1(a).

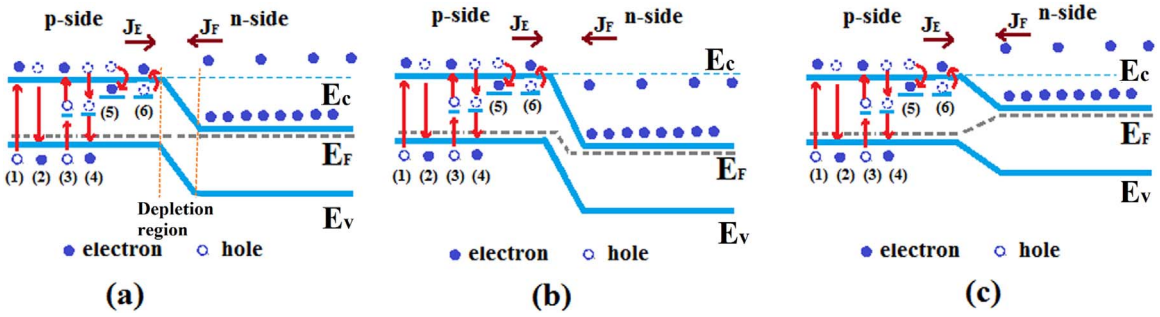

Fig. 2. The generation and annihilation of electrons in a c-Si SC under different bias-voltage conditions. (a) zero bias voltage, (b) reverse bias voltage and (c) forward bias voltage.

the distribution of electrons in the n-type region follows Fermi statistical law and there always have a small group of electrons, whose kinetic energy have exceeded the E_C value of the p-type region. These electrons, which can overcome the potential barrier to travel across the depletion region and enter the p-type region, produce the diffusion current (i.e., the current represented by J_F in Fig. 2); At the same time, a small group of electrons in both n-type and p-type regions are thermally excited from the valence band to the conduction band and those electrons in p-type region, which move to the edge of the depletion region under the action of the concentration gradient, will be pulled to n-type region by the electric field of depletion region and generate the drift current in the depletion region(i.e., the current represented by J_E in Fig. 2). In the absence of bias and under balanced state condition (as shown in Fig. 2(a), $J_F = J_E$; under the reverse bias(as shown in Fig. 2(b)), the barrier height of depletion region will increase and $J_F < J_E$ for the number of the electrons beyond the E_C line in the n-type region decrease; under the forward bias (as shown in Fig. 2(c)), the barrier height of depletion region will decrease and $J_F > J_E$ for the number of the electron beyond the E_C line in the n-type region increase.

Minority carriers are susceptible to impurities and defects. The influences of impurities and defects are also discussed by taking the electron in the p-type region as an example. Fig. 2 only shows the transition processes associated with the electrons. In Fig. 2, the up arrows of (1), (3) and (6) represent the transition processes of electrons from valence band and defect levels to conduction band; the down arrows of (2), (4) and (5) represent the transition processes of electrons from conduction band to valence band and defect levels. The processes of (1) and (2) belong to the direct transition of electrons between the conduction and valence band, which are the main transition process of electrons in a pure silicon material; the processes of (3) and (4) represent the transition of electrons between the conduction and valence band with the help of the energy level close to the central position of the band gap; the transition process of (5) and (6) represent the transition of electrons between the conduction and acceptor level. According to the difference between the capture capability for electron and holes (i.e. σ_n and σ_p), where σ represents capture cross section and subscripts of n and p denote electron and hole, respectively, impurities and defects can be divided into three kinds, i.e. the acceptor-like ($\sigma_p > \sigma_n$), donor-like ($\sigma_n > \sigma_p$) and recombination-center-like ($\sigma_n \approx \sigma_p$) impurities and defects. The energy levels for these acceptor-like, donor-like and recombination-center-like impurities and defects are close to the bottom of the conduction band, the top of the valence band and the center of the band gap, respectively. In our calculation, these defect states are described by the following formulas [23–25]:

$$D_A(E) = N_A \exp\left(\frac{E - E_c}{\tau_A}\right) \quad (1)$$

$$D_D(E) = N_D \exp\left(\frac{E_v - E}{\tau_D}\right) \quad (2)$$

$$D_G(E) = N_G \exp\left[-\left(\frac{E_G - E}{\tau_G}\right)^2\right) \quad (3)$$

where N_A, N_D and N_G represent the state densities of the donor-like, acceptor-like and recombination-center-like energy levels, respectively; E_C, E_V and E_G are the energy at the bottom of conduction band, the top of valence band and the recombination center, respectively (the energy at the top of valence band is usually defined as 0 eV, and the energy for other energy levels take it as a reference.); τ_A、τ_D and τ_G are the characteristic decay constants for three kinds of defect states. The distribution function f of carriers at the defect energy level is defined as [23–25] :

$$f_l = \frac{v_l \sigma_l n_l + v_m \sigma_m n_i \exp\left(\frac{E_l - E}{kT}\right)}{v_n \sigma_n \left(n + n_i \exp\left(\frac{E - E_i}{kT}\right)\right) + v_p \sigma_p \left(p + n_i \exp\left(\frac{E_i - E}{kT}\right)\right)} \quad (4)$$

where v represents thermal motion velocity; σ represents capture cross section; n and p are the concentrations of electrons and holes, respectively; the subscripts of n and p are corresponding with electrons and holes, respectively; ni is intrinsic carrier concentration; Ei is the energy level at the center of band gap; k is the Boltzmann constant; T is Kelvin temperature (The Kelvin temperature of 300 K is used in this paper); for a donor-like defect, l and m represent the parameters of holes and electrons, respectively; for an acceptor-like defects, l and m represent the parameters of electron and hole, respectively.

The electrode form at the front surface is another important factor of influencing the dark I-V characteristic curve. Due to the uneven dopant distribution at the front surface of a c-Si SC (shown in Fig. 1(b)), the transportation processes of holes diffused from p-type region to n-type region, will be obviously influenced by the resistivity distribution in the thin layer of n-type region and the S value. The influences of the resistivity distributions on the dark I-V curves of c-Si SCs have received extensive attention [1,11,14], but those of the S values have not attracted much attention. In fact, once a good ohmic contact has been formed between the electrode metal and the silicon material and the resistivity distribution in the thin layer of n-type region is definite, the S value determines the transport path lengths of holes in n-type region. Fig. 3 shows the schematic diagram that under the forward bias, the transportation processes of holes (majority carriers) generated in p-type region go through the depletion region and reach the n-type region(minority carrier). As shown in Fig. 3, the movements of the holes in p-type region and far from the position of pn junction are mainly driven by the concentration gradient, and they will move toward pn junction; those holes, which reach the boundary of pn junction, will be slowed down by the built-in electric field in depletion

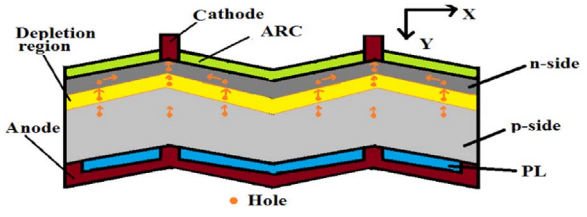

Fig. 3. Under the forward bias, the schematic diagram that the hole in p-type region goes through the pn junction and moves toward the electrode.

region and become minority carriers in the n-type region, which will be recombined by electrons injected by electrode. The holes under the electrode can be rapidly recombined by the high- concentration electrons injected by the electrode, but those far away from the electrode will require a relatively long path to be recombined by the electrons injected by the electrode because these positions have relatively lower concentrations of injected electrons. For this reason, the S value must exert an effect on the dark I-V characteristic curve of a c-Si SC.

2.3. Simulation method

In our simulation, the basic semiconductor-device equations are solved by two dimensional finite difference method exploited by our group [16,17], where the numbers of grid along X and Y direction are100 and 2000 respectively, and the space step in each direction is 0.1 μm. The impurity distribution in Fig. 1 is introduced into our program and other material parameters are selected as follows [23–26]: E_c = 1.08 eV, N_c = 2.8×10^{19}/cm^3, E_v = 0 eV, N_v = 2.8×10^{19}/cm^3, μ_n = 1000 cm^2/V.s, μ_p = 500 cm^2/V.s, $\tau_n = \tau_p$ = 1×10^{-3}s, τ_A = 0.05 eV, τ_D = 0.05 eV, τ_G = 0.1 eV,$E_A = E_D$ = 0.05 eV and E_G0.4 eV, where E_c, N_c, E_v and N_v are the energies and state densities at the bottom of conduction band and on the top of the valence band, respectively; μ_n, μ_p, τ_n and τ_p are the electron mobility, hole minority, minority electron lifetime and minority hole lifetime, respectively; τ_A, τ_D,τ_G, E_A, E_D and E_G are the characteristic decay constants and the energies of defect levels of three types of defects, respectively. According to the values of the above material parameters, the values of τ_n and τ_p represent the c-Si material without any defects and their values will vary with the properties of impurities and defects. Due to the complex influences of impurities and defects on the dark I-V characteristic curve, in our simulation, we only discuss the influence of one type of impurities and defects by assuming the values of the capture cross sections and densities of other types of impurities and defects are equal to 1 × 10^{-21} cm^2 and 1 × 10^{-5} cm^3, respectively, which mean that their capturing effects are very weak. In addition, according to the difference between the values of the capture cross section of electron (i.e. σ_n) and hole (i.e. σ_p), we assume that $\sigma_{nG}\approx\sigma_{nG}$, which will be denoted by σ_G in our simulation; $\sigma_{nA} = \sigma_{pD}$ = 1 × 10^{-21} cm^2 and the values of σ_{pA} andσ_{nD} are much larger than 1 × 10^{-21} cm^2, which means that the acceptor-like and donor-like defects only have the capturing effects on the holes in n-type region and electrons in p-type region, respectively. Here σ_{nA}, σ_{pA},σ_{nD}, σ_{pD}, σ_{nG} and σ_{nG} are the capture cross section of the acceptor-like, donor-like and recombination-center -like impurities and defects, respectively.

The ideal diode model, which will be used to analyze the dark I-V characteristic curve of a c-Si SC obtained, can be expressed as [1]:

$$J(V_A) = J_0^{eff}(\exp\frac{V_A}{n_{eff}V_T} - 1) - J_{sc} \quad (5)$$

where the V_A, V_T , J_{sc}, n_{eff} and J_0^{eff} are the anode voltage, thermal voltage, short-circuit current density under illumination, ideal factor and reverse saturation current density, respectively. When the temperature is certain and $J(V_A) >> J_0^{eff}$ (V_A takes a lager value), the natural logarithm of $J(V_A)$ is linear with V_A and the slope of the straight line is related to the n_{eff} value. The ideal diode model with n_{eff} = 1 is usually called the standard diode model, which represents that the current flowing through a pn junction is mainly composed by the diffusion current (forward bias) or drift current (reverse bias).

3. Results and discussions

3.1. The influences of the S and N_b values on the dark I-V characteristic curve

Fig. 4 shows the dark I-V characteristic curve of the c-Si SC varying with the S and N_b values, where the value of N_b, which denote the substrate doping concentration, is 5×10^{16}/cm^3 in Fig. 4(a). In Fig. 4(a), the size of pyramid, the diffusion condition and the meanings of M and S symbols are the same with those used in Fig. 1. As shown by Fig. 4(a), the dark current of the dark I-V characteristic curves with the fixed values of M and S will be almost constant with the reverse bias voltage increasing in a wide range of the reverse bias; under the same reverse bias voltage, the dark current decreases with the increasing of M value and increases with the increasing of S value; the dark I-V characteristic curves with the same M and S values can be in good accordance with the ideal diodedark I-V characteristic curve with n_{eff}=1 in a wide range of forward bias voltage (the area between line A and line B); the dark current values increase with the increasing of M and S values under the same forward bias voltage. Fig. 4(a) shows that under the same reverse bias voltage, the deviations between the dark I-V characteristic curves of the c-Si SC with the same S and different M values in the area between line A and line B are very close to each other, so the study on the dark I-V characteristic curve of a actual c-Si SC with multiperiod pyramid can be realized by using that of the corresponding c-Si SC with a single pyramid. In the following discussion, we will adopt the single pyramid model (i.e. M = 1) to discuss the properties of the dark and illuminated I-V characteristic curves.

The dark I-V characteristic curves of the c-Si SC with M = 1 and S = 0.5 varying with the values of N_b are shown in Fig. 4(b), where the size of pyramid and diffusion condition are the same with those used in Fig. 1. Under the same process condition, the changes of the N_b values will influence the properties of the pn junction fabricated (such as junction depth, the width of depletion region) and the sheet resistance beneath the electrode. As shown by Fig. 4(b), the dark current densities under the same bias voltage decrease with the increasing of N_b values, but the amplitude variations of the dark current densities are very small; the dark I-V characteristic curves can be in good accordance with the n_{eff}=1 curve in a wide range of forward bias.

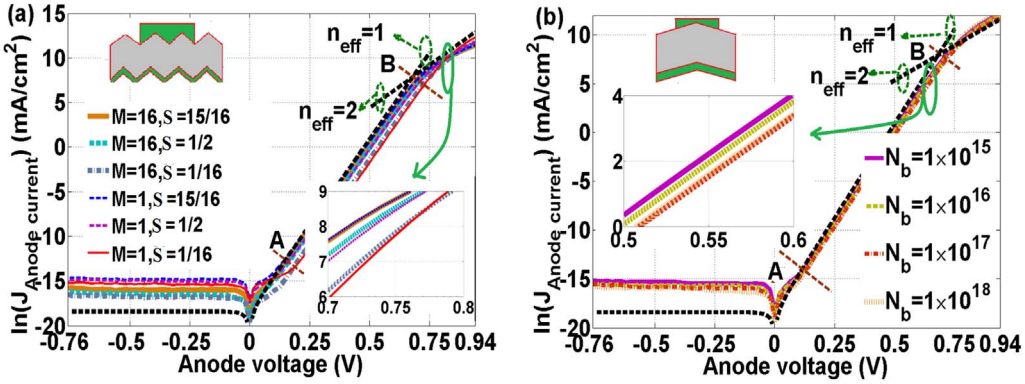

Fig. 4. The dark I-V characteristic curves varying with the values of S and N_b, where (a) and (b) are corresponding to the values of S and N_b, respectively.

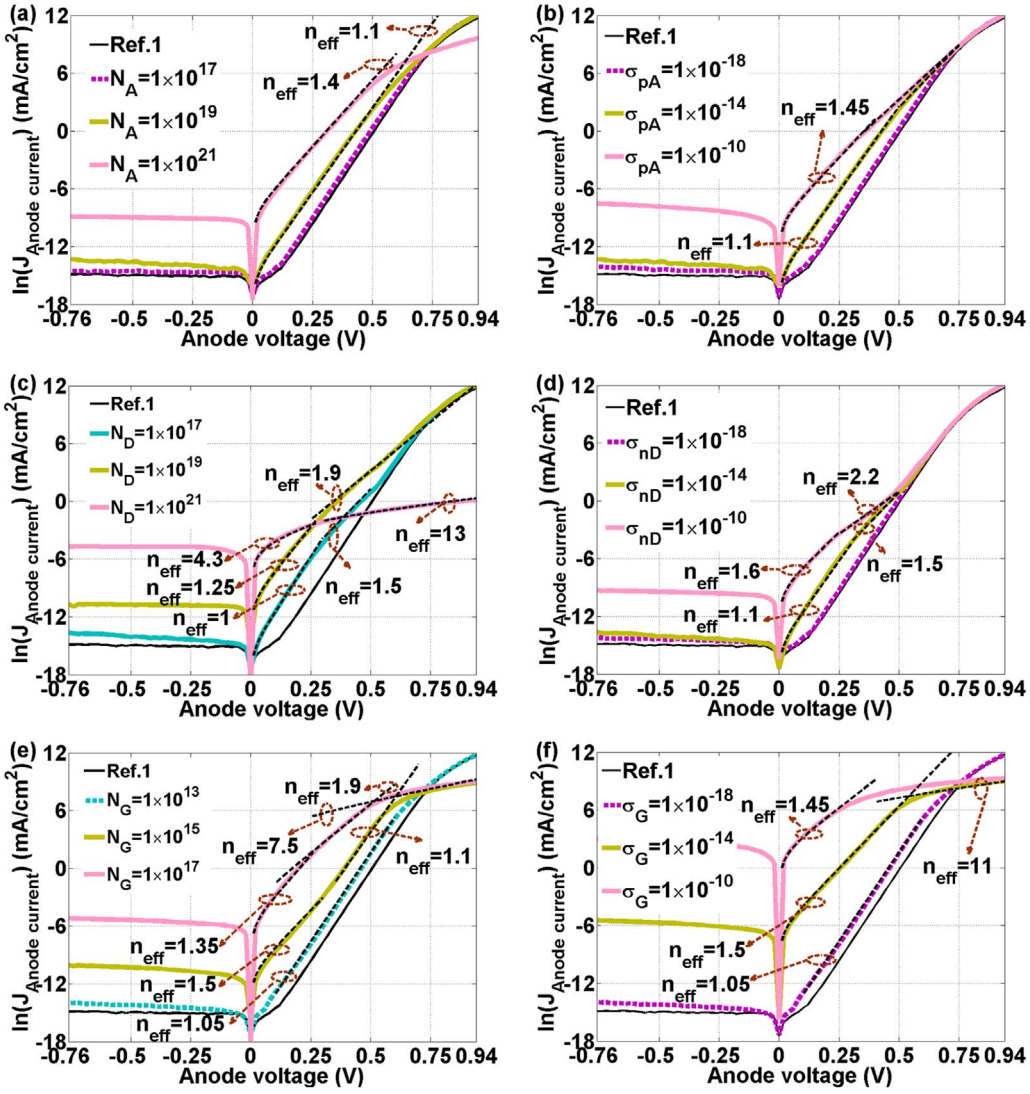

Fig. 5. The influences of the impurities and defects inside c-Si materials on the dark I-V characteristic curves, where (a), (b), (c),(d), (e) and (f) are the variations of the dark I-V characteristic curves with N_A,σ_{pA}, N_D,σ_{nD}, N_G and σ_G respectively.

3.2. The influence of the properties of the impurity and defect within a c-Si SC on the dark I-V characteristic curve

Fig. 5 shows the dark I-V characteristic curves varying only with the properties of the impurities and defects inside the c-Si SC, where the structure and process parameters of the c-Si SC are the same as those used in Fig. 1, but the S value is chosen as 0.5. In Fig. 5, the Ref. [1] curve represents the I-V characteristic curve of the c-Si SC with $\tau_n = \tau_p = 1 \times 10^{-3}$s; the line denoted by n_{eff} represents the ideal diode I-V characteristic curve with n_{eff} equal to a certain value. Fig. 5(a), Fig. 5(c) and Fig. 5(e) show the dark I-V characteristic curves varying with the N_A, N_D and N_G values, respectively, where the σ_{pA}, σ_{nD} and σ_G are all set to 1×10^{-14} cm^2 [4,5,7]. Fig. 5(b), Fig. 5(d) and Fig. 5(f) show the dark I-V characteristic curves varying with the σ_{pA}, σ_{nD} and σ_G values, respectively, where $N_A = 1\times10^{19}$/cm^3 in Fig. 5(b), $N_D = 1\times10^{17}$/cm^3 in Fig. 5(d) and $N_G = 1\times10^{17}$/cm^3 in Fig. 5(f).

As shown by Fig. 5, the dark current values increase with the increasing of the N_A, N_D, N_G, σ_{pA}, σ_{nD} and σ_G values in the range of the reverse bias voltage and small forward bias voltage; when the N_A, N_D, N_G, σ_{pA}, σ_{nD} and σ_G values are very small, the dark current values of the c-Si SC are close to those dark current values given by Ref. [1] curve in a wide range of forward bias, while when the N_A, N_D, N_G, σ_{pA}, σ_{nD} and σ_G values are very big, the dark current values of the c-Si SC will deviate obviously from the dark current values given by Ref. [1] curve. For a certain capture cross section or a certain defect state density, there exists a minimum value (i.e. threshold) for the N_A, N_D or N_G values or for the σ_{pA}, σ_{nD} or σ_G values, where the influence of the corresponding impurities and defects on the dark I-V characteristic curve of the c-Si SC can be neglected. Here, we use N_{AT}, N_{DT}, N_{GT}, σ_{pAT}, σ_{nDT}, σ_{GT} to denote the threshold of N_A, N_D, N_G, σ_{pA}, σ_{nD} and σ_G, respectively. As shown by Fig. 5, when $\sigma_{pA} = 1 \times 10^{-14}$ cm^2, $\sigma_{nD} = 1 \times 10^{-14}$ cm^2 and $\sigma_G = 1 \times 10^{-14}$ cm^2, $N_{AT} = 1 \times 10^{17}$/cm^3, $N_{DT} = 1 \times 10^{15}$/cm^3 and $N_{GT} = 1 \times 10^{13}$/cm^3, respectively and when $N_A = 1 \times 10^{19}$/cm^3, $N_D = 1 \times 10^{17}$/cm^3 and $N_G = 1 \times 10^{17}$/cm^3, $\sigma_{pAT} = 1 \times 10^{-18}$ cm^2, $\sigma_{nDT} = 1 \times 10^{-18}$ cm^2, $\sigma_{GT} = 1 \times 10^{-14}$ cm^2, respectively. When the values of N_A, N_D, N_G, σ_{pA}, σ_{nD} and σ_G are equal to or lower than their corresponding thresholds, the dark I-V characteristic curve will be close to the Ref. [1] curve and quite insensitive to the changes of N_A, N_D, N_G, σ_{pA}, σ_{nD} and σ_G values.

The dark I-V characteristic curves can be further analyzed by using ideal factor. As shown by Fig. 5, the dark I-V characteristic curves of the c-Si SC have the same n_{eff} values with the Ref.1 curve, when the values of N_A, N_D, N_G, σ_{pA}, σ_{nD} and σ_G are smaller than their corresponding thresholds; in the forward bias range with V < 0.5 V, the dark I-V characteristic curves can be fitted by a ideal dark I-V characteristic curve with a single n_{eff} value for different N_A and σ_{pA}

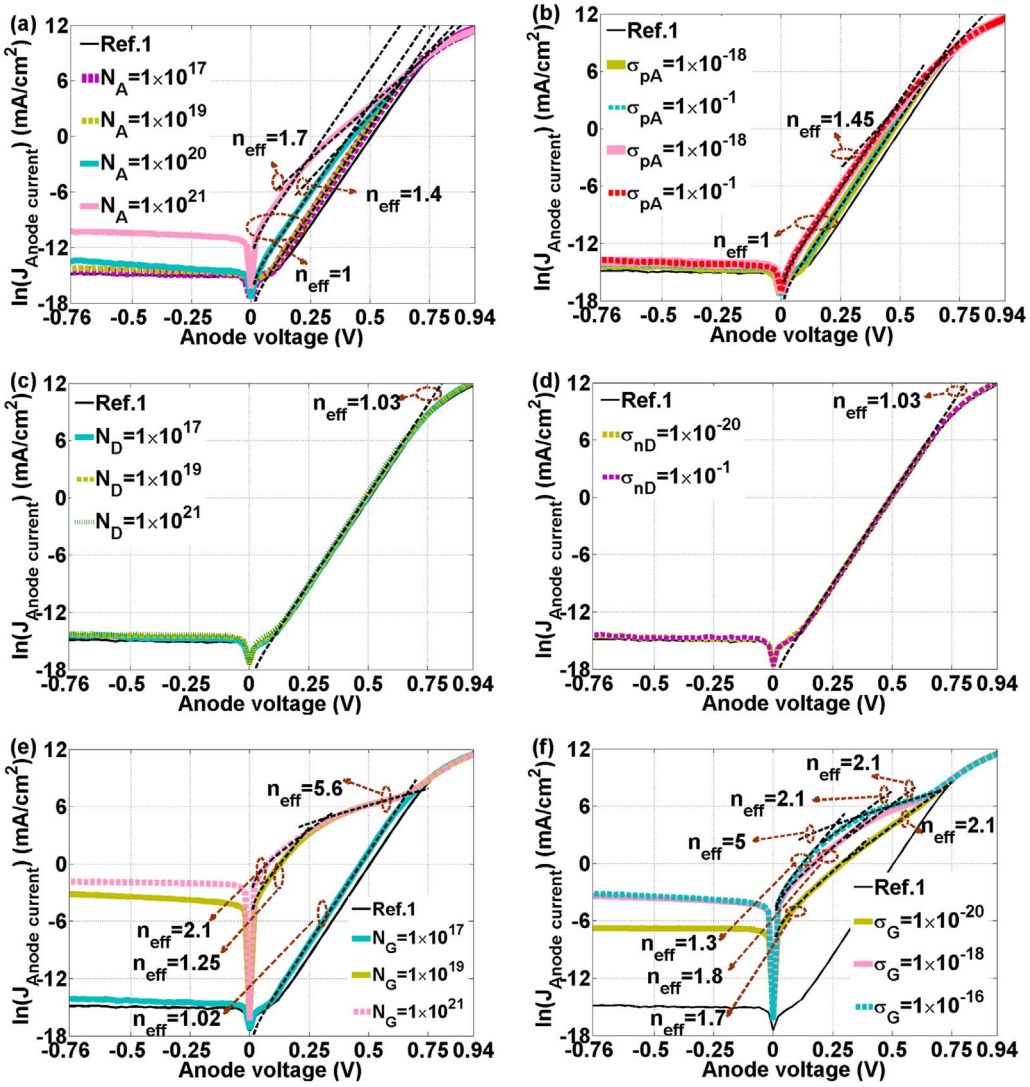

Fig. 6. The influence of surface impurities and defects on the dark I-V characteristic curves, where (a), (b), (c),(d), (e) and (f) are the variations of the dark I-V characteristic curves with N_A,σ_{pA}, N_D,σ_{nD}, N_G and σ_G respectively.

values (i.e. the acceptor-like impurities and defects) and by two ideal dark I-V characteristic curves with two different n_{eff} values for different N_D, σ_{nD}, N_G and σ_G values (i.e. the donor-like and recombination-center-like impurities and defects); the dark I-V characteristic curves varying with the N_D and σ_{nD} values, mainly lie in the range of small forward bias and they will turn into the ideal dark I-V characteristic curve with n_{eff} = 1 in the range of forward bias from 0.5 V to 0.75 V; the variations of the dark I-V characteristic curves with the N_G and σ_G values, occur in a wide range from 0.1 V to 0.75 V and the differences between those dark I-V characteristic curves and the ideal dark I-V characteristic curve with n_{eff} = 1.

3.3. The influence of the properties of the impurities and defects on the surface of a c-Si SC on the dark I-V characteristic curves

Fig. 6 shows the dark I-V characteristic curves of the c-Si SC varying only with the properties of the impurities and defects on its surfaces, where the structure and process parameters of the c-Si SC are the same as those used in Fig. 1, but the S value is also chosen as 0.5. The symbols in Fig. 6 have the same meanings with those in Fig. 5. The values σ_{pA}, σ_{nD} and σ_G in Figs. 6(a), (c) and (e) are all set to 1 × 10^{-14} cm^2 and the values of N_A, N_D, N_G in Figs. 6(b), (d) and (f) are all set to 1 × $10^{19}/cm^3$. Due to the differences between the dark I-V characteristic curves with different σ_{pA} values very small, we have also added the dark I-V characteristic curve with N_A = 1 × $10^{20}/cm^3$ in Fig. 6(b) to show more accurately the influences of the σ_{pA} values on the dark I-V characteristic curves. In addition, due to the differences between the dark I-V characteristic curves with N_D = 1 × $10^{20}/cm^3$ and N_D = 1 × $10^{19}/cm^3$ very small, the dark I-V characteristic curve with N_D = 1 × $10^{20}/cm^3$ is not given in Fig. 6(c).

Fig. 6 shows that the variations of the dark I-V characteristic curves only with the values of σ_{pA}, N_D and σ_{nD} are very small, which means the values of σ_{pA}, N_D and σ_{nD} have insignificant influence on the dark I-V characteristic curves; the influences of the N_A and N_G values on the dark I-V characteristic curves have obvious threshold effects, where N_{AT} = 1 × $10^{19}/cm^3$ and N_{GT} = 1 × $10^{17}/cm^3$; the values of σ_G have a large influence on the dark I-V characteristic curves. The influences of the N_A, N_D, N_G, σ_{pA}, σ_{nD} and σ_G values on the dark I-V characteristic curves of the c-Si SC in the range of the forward bias from 0.1 V to 0.5 V, can be further analyzed by the values of n_{eff}: with the increasing of the N_A and σ_{pA} values, the dark I-V characteristic curves can be fitted by two ideal dark I-V characteristic curves, where the n_{eff} value of the ideal dark I-V characteristic curve under the smaller bias is equal to 1; with the increasing of the N_G and σ_G values, the dark I-V characteristic curves can be fitted by two or three ideal dark I-V characteristic curves, where the n_{eff} values of these ideal dark I-V characteristic curves will

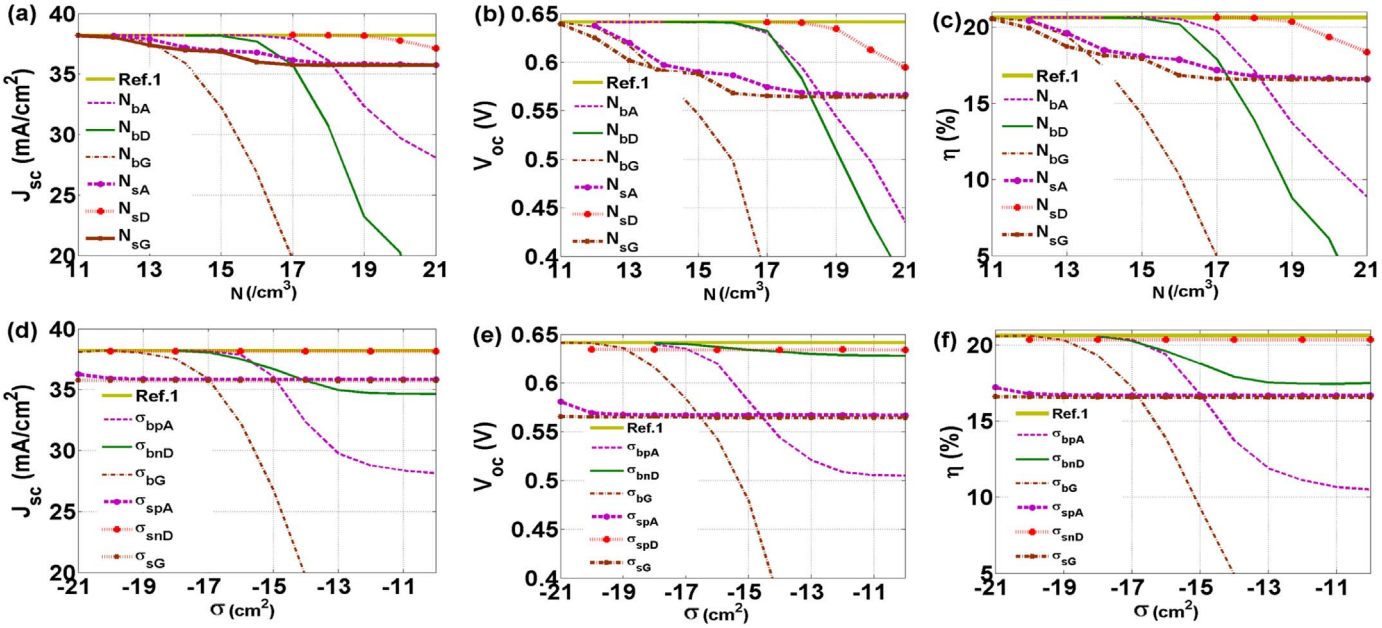

Fig. 7. The influences of the properties of impurities and defects on the output parameters of a typical c-Si SC, where the horizontal axis denoted by N and σ represent the state density and capture cross section for different types of impurities and defects, respectively.

increase first and then decrease to 1 under the bias near 0.7 V.

3.4. The influence of the properties of impurities and defects on the output parameters of a c-Si SC

Fig. 7 shows that the influence of the properties of the impurities and defects on the short-circuit current(J_{SC}), open-circuit voltage(V_{OC}) and efficiency(η), where the subscripts of b and s used by the legends in each figure, denote the impurities and defects inside and on the surface of the c-Si SC, respectively, other subscripts have the same meanings with those used in Figs. 5 and 6 and the straight lines of Ref. [1] in each figure are the corresponding output parameters of the Ref. [1] curves used in Figs. 5 and 6. In our simulation, the structure and process parameters of the c-Si SC except the S value, are the same as those used in Figs. 5 and 6. According to the relationship between the S value and dark I-V characteristic curve given by in Fig. 4(a) and the practical parameters of fine grid used by those c-Si SC in the SC market, here we select the S value as 0.0375, which can correspond with the case that the width of fine grid and the minimum distance between two fine grids are 75 μm and 2 mm, respectively. The method for changing the values of N and σ is the same with those used in Figs. 5 and 6. In order to fully show the variations of the output parameters of the c-Si SC with the properties of impurities and defects, we have also extended the value range of the N and σ parameters in our calculation.

Figs. 7(a), (b) and (c) show that when the N value for each type of impurities and defects is larger than a certain value, the values of J_{sc}, V_{oc} and η will all decrease with the increasing of N value; under the condition of $N \leq 10^{13}/cm^3$(low defect density), the values of J_{sc}, V_{oc} and η are discernibly influenced by the N_{bG}, N_{sA} or N_{sG} values, especially by the N_{sG} values; under the condition of $10^{13}/cm^3 < N \leq 10^{17}/cm^3$(medium defect density), with the increasing of N values, the influences exerted by the N_{bG} values will increase rapidly, those exerted by the N_{sA} or N_{sG} values will become more and more obvious and those exerted by the N_{bD} or N_{bA} values begin to emerge; under the condition of $10^{17}/cm^3 < N \leq 10^{19}/cm^3$(high defect density), the influences of the N_{sA} or N_{sG} values will become insensitive to the increasing of N values, but with the increasing of N values, the influences of the N_{bA}, N_{bD}, N_{bG} values will further increase and those of the N_{bA} or N_{bD} values will finally exceed those of the N_{sA} or N_{sG} values; under the condition of $N > 10^{19}/cm^3$(ultrahigh defect density), the values of N_{bA}, N_{bD}, N_{bG}, N_{sA}, N_{sD} or N_{sG} will all have obvious influences on the values of J_{sc}, V_{oc} and η, but the influences of N_{bA}, N_{bD} and N_{bG} are larger than those of N_{sA}, N_{sD} and N_{sG}.

Figs. 7(d), (e) and (f) show that: with the σ value lager than a certain value and the increasing of σ value for each type of impurities and defects, the influences of the σ_{bpA}, σ_{bnD} and σ_{bG} values will increase gradually, but those of the σ_{spA}, σ_{snD} and σ_{sG} values will almost keep unvaried; under the condition of $\sigma \leq 10^{-17}$ cm^2 (weak capturing effect), the value of J_{sc}, V_{oc} and η are mainly influenced by the σ_{spA} and σ_{sG} values; under the condition of 10^{-17} cm^2 < N≤10^{-13} cm^2(medium capturing effect), with the increasing of the σ value, the values of J_{sc}, V_{oc} and η are mainly influenced by the σ_{bG} values and the influence of σ_{bpA} will gradually exceed those of σ_{spA} and σ_{sG}; under the condition of $\sigma > 10^{-13}$ cm^2(strong capturing effect), with the increasing of the σ value, the values of J_{sc}, V_{oc} and η are mainly influenced by σ_{bpA} and σ_{bG}; different σ_{snD} values have basically no influence on the J_{sc}, V_{oc} and η values; the changes of the σ_{bnD} values have very weak influence on the V_{oc} value.

Fig. 7 also shows that in addition to the σ_{snD} value, other parameters, such as N_{bA}, N_{bG}, N_{sA}, σ_{spA} and σ_{sG}, all have threshold effects; the values of J_{sc}, V_{oc} and η are insensitive to the changes of the σ values for different surface impurities and defects. Here we can draw conclusions that in order to fabricate the c-Si SCs with high efficiency, the goals of $N_{bA} < 10^{17}/cm^3$, $N_{bD} < 10^{15}/cm^3$, $N_{bG} < 10^{12}/cm^3$, $\sigma_{bpA} < 10^{-17}$ cm^2, $\sigma_{bnD} < 10^{-17}$ cm^2 and $\sigma_{bG} < 10^{-20}$ cm^2 must be first accomplish by various process techniques and then the values of N_{sA}, N_{sD} and N_{sG} must be drastically reduced to the level of $N_{sA} < 10^{12}/cm^3$、$N_{sD} < 10^{19}/cm^3$、$N_{sG} < 10^{11}/cm^3$ by using various effective surface passivation technologies.

3.5. The judgment criterions of the properties of impurities and defects by using the dark I-V characteristic curves

Based on the dark I-V characteristic curves shown in Figs. 5 and 6, the judgment criterions of the properties of impurities and defects can be given as following:

1) The dark I-V characteristic curves in the range of reverse bias can provide us with the information about the relative values of the N_A, N_D, N_G, σ_{pA}, σ_{nD} or σ_G value, i.e., the larger the dark current value

of a c-Si SC under the same reverse bias is, the larger the N_A, N_D, N_G, σ_{pA}, σ_{nD} or σ_G value will be.

2) Under the same forward bias, the larger the dark current is, the larger the value of N or σ for the same kind of impurities and defects will be.
3) In the range of higher forward bias (the anode voltage is larger than 0.75 V), if the n_{eff} value for a dark I-V characteristic curve is larger than 2, it means that the impurities and defects, which can exert a great influence on the dark I-V characteristic curve, lie inside the c-Si material and the value of N_A, N_D, N_G or σ_G is much larger than its corresponding threshold (i.e., N_{AT}, N_{DT}, N_{GT} or σ_{GT}).
4) The important properties of impurities and defect can be analyzed by the information offered by the dark I-V characteristic curve in the range of forward bias from 0.1 V to 0.75 V, i.e.: ① If the dark I-V characteristic curve in this range can be fitted only by an ideal diode I-V characteristic curve with the n_{eff} value equal to 1, the values of N_A, N_D, N_G, σ_{pA} and σ_{nD} for the impurities and defects inside and on the surface of the c-Si SC are all close to or smaller than their corresponding thresholds (i.e. the values of N_{AT}, N_{DT}, N_{GT}, σ_{pAT}, σ_{nDT} and σ_{GT}); ② If the dark I-V characteristic curve in the subrange from 0.1 V to 0.5 V can be fitted only by an ideal diode I-V characteristic curve with the n_{eff} value larger than 1, it means that the impurities and defects, which can exert a discernible influence on the dark I-V characteristic curve, are acceptor-like impurities and defects and lie inside the c-Si material; ③ If the dark I-V characteristic curve in this range can be fitted by three ideal diode I-V characteristic curves with three different n_{eff} values (assuming that with the increase of the anode voltage, the values of n_{eff} are denoted by n_{eff1}, n_{eff2} and n_{eff3}, respectively), there will have four situations: when $n_{eff1}=1$, $n_{eff2}>1$ and $n_{eff3}=1$, the impurities and defects with discernible influences are acceptor-like impurities and defects and lie on the surface of the c-Si material; when $n_{eff1}>1$, $n_{eff2}>n_{eff1}$ and $n_{eff3}=1$, the impurities and defects with discernible influences are donor-like impurities and defects and lie inside the c-Si material; when $n_{eff1}>1$, $n_{eff2}>n_{eff1}$, $n_{eff3}>n_{eff2}$ and $n_{eff3}>2$, the impurities and defects with discernible influences are recombination-center-like impurities and defects and lie inside the c-Si material; when $n_{eff1}>1$, $n_{eff2}>2$, $n_{eff3}=2$ and an obvious point of inflection appear on the dark I-V characteristic curve in the vicinity of 0.75 V, the impurities and defects with discernible influences are recombination-center-like impurities and defects and lie on the surface of the c-Si material.
5) The recombination-center-like impurities and defects on the surface of the c-Si material can strongly influence the dark I-V characteristic curves in the range of forward bias from 0.1 V to 0.7 V, but in the range with forward bias larger than 0.7 V, these dark I-V characteristic curves will coincide with the Ref1 curve; the recombination-center-like impurities and defects inside the c-Si material can influence obviously the dark I-V characteristic curves in the whole range of forward bias and in the range with forward bias larger than 0.7 V, the values of n_{eff} for these dark I-V characteristic curves are larger than 2.

4. Conclusion

The influences of different factors on the dark I-V characteristic curves of a c-Si SC are analyzed in detail, and a lot of important conclusions are obtained:

The larger the S value is, the greater the dark current value under the same bias will be; the smaller the doping concentration of substrate is, the larger the dark current value under the same bias will be; the influences of the variations of the parameters for the acceptor-like, donor-like and recombination-like impurities and defects on the dark I-V characteristic curve, show obvious threshold effects; the donor-like impurities and defects on the surface of a c-Si SC will weak affect on its dark I-V characteristic curves, but the acceptor-like and recombination-like impurities and defects on the surface of a c-Si SC will strongly influence on its dark I-V characteristic curve; under the low and medium defect density, the recombination-like and acceptor-like impurities and defects on the surface of a c-Si SC and the recombination-like impurities and defects inside the c-Si SC are the main factor, which can strongly influence on the output parameters of the c-Si SC; under the high and ultrahigh defect density, all kinds of impurities and defects can exert discernible influences on the output parameters of a c-Si SC; when the capturing effects of impurities and defects are very weak, the acceptor-like and recombination-like impurities and defects on the surface are the main factor that have strong influences on the output parameters of c-Si SC; when the capturing effects of impurities and defects are strong, the acceptor-like and recombination-like impurities and defects inside the c-Si SC have obvious influences on the output parameters of a c-Si SC; the properties of impurities and defects can be analyzed and judged by using the ideal factor of the dark I-V characteristic curve of a c-Si SC.

Acknowledgments

This work was supported by program for National Natural Science Foundation of Chin (No: 61575029), Liaoning Natural Science Foundation of China (No: 201602008).

References

[1] O. Breitenstein, S. Ribland, A two-diode model regarding the distributed series resistance, Sol. Energy Mater. Sol. Cells 110 (2013) 77–86.
[2] D. WBrown, M. Abbas, A. Ginart, et al., Turn-Off time as an early indicator of insulated gate bipolar transistor Latch-up, IEEE Trans. Power Electron. 27 (2) (2012) 479–489.
[3] Q. Huang, X. Zhang, J. Xia, et al., Systematic investigation of silicon digital 1×2 electro-optic switch based on a microdisk resonator through carrier injection, Appl. Phys. B: Lasers Opt. 105 (2011) 353–361.
[4] M. Al-Amin, J.D. Murphy, Increasing minority carrier lifetime in as-grown multi-crystalline silicon by low temperature internal gettering, J. Appl. Phys. 119 (23) (2016) (235704-1-235704-14).
[5] G. Martins, R.S. Bonilla, T. Burton, et al., Minority carrier lifetime improvement of multicrystalline silicon using combined saw damage gettering and emitter formation, Solid State Phenom. 242 (2016) 126–132.
[6] H. Inchan, R.M. Christopher, N.C. Greenham, Drift-diffusion modeling of photo-current transients in bulk heterojunction solar cells, J. Appl. Phys. 106 (9) (2009) 094506–094516.
[7] R.V.K. Chavali, B. Ray, M.A. Alam, Correlated nonideal effects of dark and light I–V characteristics in a-Si/c-Si heterojunction solar cells, IEEE J. Photovolt. 4 (3) (2014) 763–771.
[8] P. Somasundaran, R. Gupta, Evaluation of shunt losses in industrial silicon solar cells, Int. J. Photo. 2016 (2016) 1–9.
[9] J. Salinger, Measurement of solar cell parameters with dark forward I-V characteristics, Acta Polytech. 46 (4) (2006) 25–27.
[10] E.Q.B. Macabebe, E.E. Dyk, Parameter extraction from dark current–voltage characteristics of solar cells, South Afr. J. Sci. 104 (2008) 401–404.
[11] O. Breitenstein, J. Bauer, A. Lotnyk, et al., Defect induced non-ideal dark I-V characteristics of solar cells, Superlattices Microstruct. 45 (2009) 182–189.
[12] O. Breitenstein, J. Bauer, P.P. Altermatt2, et al., Influence of defects on solar cell characteristics, Solid State Phenom. 156–158 (2010) 1–10.
[13] S. Tutashkonko, A.K. Cachopo, C. Boulord, et al., Light induced silver and copper plating on silver screen-printed contacts of silicon solar cells, Opto-Electron. Rev. 19 (3) (2011) 301–306.
[14] L. Derbali, H. Ezzaouia, Vanadium-based antireflection coated on multicrystalline silicon acting as a passivating layer, Sol. Energy 86 (5) (2012) 1504–1510.
[15] A.K. Biswas, S. Biswas, A. Chatterjee, et al., The injected dark current of a p+n and a p+n n+ silicon solar cell taking into account the narrowing of band gap due to heavy doping, Int. J. Renew. Energy Res. 6 (1) (2016) 10–14.
[16] X. Lu, Z. Wang, Y. Zhao, et al., The output parameter and temperature distribution characteristics of c-Si SC varying with temperature, Sci. Sin. Technol. 46 (5) (2016) 458–466.
[17] Y. Zhao, Z. Wang, P. Zhang, et al., Application of finite difference method in simulation of solar cell, Laser Optoelectron. Progress. 53 (2016) 030401.
[18] J. Zhao, A. Wang, M.A. Green, 24.5% efficiency silicon PERT cells on MCZ substrates and 24.7% efficiency PERL cells on FZ substrates [J], Progress in Photovoltaics: Research and Applications, 19997, 471-474.
[19] V.K. Singh, J. Nagaraju, Effect of diffusion parameters on the efficiency of c-Si solar cell, Adv. Mater. Lett. 6 (7) (2015) 600–606.
[20] J. Zhao, A. Wang, M.A. Green, 24.5% efficiency silicon PERT cells on MCZ substrates and 24.7% efficiency PERL cells on FZ substrates, Progress. Photovolt.: Res. Appl. 7 (1999) 471–474.
[21] Y. Liu, Y. Sun, W. Liu, et al., Novel high-efficiency crystalline-silicon- based

compound heterojunction solar cells: hct (heterojunction with compound thin-layer), Phys. Chem. Chem. Phys. 16 (29) (2014) 15400–15410.
[22] D.B.M. Klaassen, A unified mobility model for device simulation - II. Temperature dependence of carrier mobility and lifetime, Solid-State Electron. 35 (7) (1992) 961–967.
[23] C.Y. Su, H.L. Hwang, Simulation and analysis of amorphous silicon image sensor having a p–i–n structure, Solid-State Electron. 35 (12) (1992) 1811–1816.
[24] A.M. Kemp, M. Meunier, C.G. Tannous, Simulations of the Amorphous Silicon Static Induction Transistor, Solid-State Electron. 32 (2) (1989) 149–157.
[25] X.D. Lu, Y. Song, Z.L. Wang, et al., Influences of properties of volume defects on dark I-V characteristics of crystalline silicon solar cell, Electron. Compon. Mater. 35 (10) (2016) 39–44.
[26] J.G. Shaw, M. Hack, Analytic model for calculating trapped charge in amorphous silicon, J. Appl. Phys. 64 (9) (1988) 4562.